BULLETIN OF THE POLISH ACADEMY OF SCIENCES
TECHNICAL SCIENCES, Vol. 69(5), 2021, Article number: e137412
DOI: 10.24425/bpasts.2021.137412

Mechanisms of plastic deformation in light high-manganese steel of TRIPLEX type

Liwia SOZAŃSKA-JĘDRASIK[1], Wojciech BOREK[2*], and Janusz MAZURKIEWICZ[2]

[1] Łukasiewicz Research Network–Institute for Ferrous Metallurgy, Department of Investigations of Properties and Structure of Materials, ul. K. Miarki 12-14, Gliwice 44-100, Poland

[2] Silesian University of Technology, Department of Engineering Materials and Biomaterials, ul. Konarskiego 18a, Gliwice 44-100, Poland

Abstract. In this scientific publication, research results of two newly developed hot-rolled Fe-Mn-Al-C (X105) and Fe-Mn-Al-Nb-Ti-C (X98) types of steel were compared. These types of steel are characterized by an average density of 6.68 g/cm^3, a value 15% lower compared to conventional structural steel. Hot rolling was carried out on a semi-industrial line to evaluate the effect of hot plastic deformation conditions with different cooling variants on the structure. The detailed analysis of phase composition as well as microstructure allows us to state that the investigated steel is characterized by an austenitic-ferritic structure with carbides precipitates. The results of the transmission electron microscopy (TEM) tests of both types of steel after hot rolling showed the occurrence of various deformation effects such as shear bands, micro bands, and lens twins in the microstructure. Based on the research undertaken with the use of transmission electron microscopy, it was found that the hardening mechanism of the X98 and X105 steel is deformation-induced plasticity by the formation of shear bands (SIP) and micro shear bands (MBIP).

Key words: Fe-Mn-Al-C steels; mechanism of plastic deformation; micro bands; shear bands; slip bands; TEM.

1. INTRODUCTION

Steel with 25–30% Mn and 9–12% Al, 0.8–1.5% C and characterized by a three-phase structure composed of austenite γ–Fe(Mn, Al, C), α–Fe ferrite (Mn, Al) and dispersion nanometric precipitates of κ–$(Fe, Mn)_3AlC$ carbide, as well as other nano and micrometric carbides related to the specific chemical composition of steel (TRIPLEX steel) [1–6]. High mechanical properties of these groups of steel are attributed to the appropriate composition of elements dissolved in the solid solution, which promotes the precipitation of κ carbide coherent with the main component of the phase, i.e., austenite. Due to the relatively high addition of Al ~ 11%, as well as Mn (18–28%) and C (0.5–1.2%), metallurgy, processing, microstructure, and deformation mechanisms of this steel differ significantly from those in traditional structural steel [3–6].

To describe the plastic deformation of Fe–Mn–Al–C steel with high stacking error energy (EBU), the concept of strain-induced plasticity by creating shear band induced plasticity (SIP), micro band induced plasticity (MBIP), or dynamic slip bands (DSBR – dynamic slip band refinement) [7–9]. The SIP effect is the main mechanism for strengthening the high-manganese steel of the TRIPLEX type (EBU ~ 110 mJ/m^2 [9]). This effect is due to the formation of intersecting shear bands in austenite. The shear bands together with evenly spaced carbides, which are coherent with the matrix, hinder the dislocation movement. The result of this effect is a high speed of strain hardening during stretching, which prevents the formation of a neck in the sample during the static tensile test, giving a high value of the $Rp_{0.2}/Rm$ ratio in the analyzed steel [3, 4, 7, 10–16].

The increase in the strengthening speed at the MBIP formation site in the above-mentioned steel is due to an increase in the total density of dislocation due to the formation of microbands [4, 7, 13–21]. With deformation of 5%, the dislocation in the slip plane along the major crystallographic directions was revealed. However, with plastic deformation of 10%, no clear formation of dislocation cells was observed, but a structure similar to Taylor's network [14].

The deformation mechanism through DSBR (Fig. 1) is characterized by a significant slip during deformation and no mechanical twins or phase transitions were observed. This mechanism causes the formation of thin slip bands in the austenite grain. During deformation, the number of slip bands increases, which results in their densification [16, 20–29]. Table 1 presents a comparison of the strengthening mechanisms in Fe-Mn-Al-C type TRIPLEX steel.

2. MATERIALS AND METHODS

The subject of the research was two plates of high-manganese steel of the TRIPLEX X98MnAlNbTi24-11 (X98) and X105MnAlSi24-11 (X105) type with high metallurgical purity, with a low concentration of gases and sulphur and phosphorus impurities (Table 2). Mischmetal (composition: cerium, lantha-

*e-mail: wojciech.borek@polsl.pl

Manuscript submitted 2021-03-11, revised 2021-04-16, initially accepted for publication 2021-04-19, published in October 2021

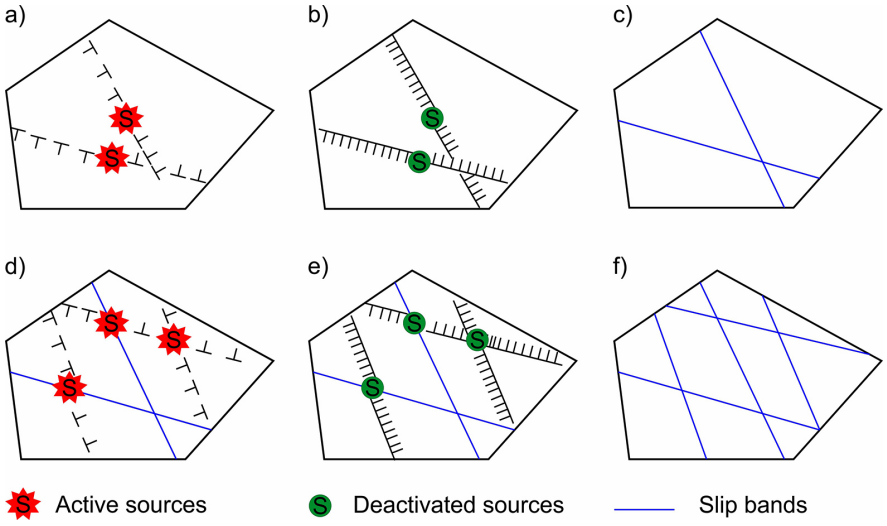

Fig. 1. Diagram of the deformation mechanism by the formation of dynamic slip bands: a) activation of dislocation sources; b, e) formation of slip planes from dislocation; c, f) slip bands; d) activation of new dislocation sources [16]

Table 1
Comparison of the strengthening mechanisms revealed in selected TRIPLEX type Fe-Mn-Al-C steel [9]

Mechanism	SIP [7]	MBIP [15]	DSBR [16]
Mechanism	Shear band induced plasticity	Micro band induced plasticity	Dynamic slip band refinement
Alloy composition	Fe-27Mn-12Al-0.9C	Fe-28Mn-10Al-1.0C	Fe-30,4Mn-8Al-1,2C
Annealing	1050°C/25 min	1000°C/60 min	1100°C/120 min
Cooling	in water	in water	in oil
Microstructure	$\gamma + 8\%\ \delta + \kappa'$ (20–30 nm)	γ + SRO[1] (<2 nm)	γ + SRO[1] (<2 nm)
Grain size γ	~ 30 µm	~ 64 µm	~ 40 µm
EBU	~ 110 mJ/m^2	~ 120 mJ/m^2	~ 85 mJ/m^2
Speed of deformation	10^{-4} 1/s	10^{-3} 1/s	5×10^{-4} 1/s
$R_{p0.2}$/A	875 MPa/58%	873 MPa/99%	900 MPa/68%

[1] Short-range orders

num, neodymium) was used to modify non-metallic inclusions in the melts. Based on preliminary tests as well as analysis of the literature data, the chemical composition of the tested steel was selected in such a way as to obtain an austenitic-ferritic structure with numerous carbides. Micro-additions of niobium and titanium in X98MnAlNbTi24-11 steel were introduced to limit grain growth as planned.

Steel was cast into a cast-iron ingot mold under an argon atmosphere. After cooling in the air, the ingot was hot worked by the free forging method, with a pressure of 300 tons at a temperature ranging from 1200 to 900°C, on a Kawazoe high-speed hydraulic press. Hot rolling was performed on the line for semi-industrial rolling simulation (LPS). The resulting plastic deformation speed for the next culverts are 9.5, 10, 10.3, and 10.1 s^{-1} with times between the passes ranging from 6 to 10 s. The end temperature of the hot rolling was 850°C [4, 6]. After hot plastic working (after rolling on a semi-industrial line – samples cut in the direction of rolling), the tests of mechanical properties were carried out on the Z100 universal testing machine by Zwick, equipped with an extensometer. The tests under dynamic conditions were performed with a rotary hammer, RSO type, manufactured by WPM Leipzig, with a strain rate of 250, 500, and 1000 s^{-1} [17]. The influence of thermo-mechanical treatment on the analyzed steel microstructure and mechanical properties was presented in the works [5, 6].

Table 2
Chemical composition of the investigated steel (wt.%)

C	Mn	Al	Si	Nb	Ti	Ce	La	Nd	P_{max}	S_{max}
Steel X98MnAlNbTi24-11 (steel X98)										
0.98	23.83	10.76	0.20	0.048	0.019	0.029	0.006	0.018	0.002	0.002
Steel X105MnAlSi24-11 (steel X105)										
1.05	23.83	10.76	0.10	–	–	0.037	0.011	0.015	0.005	0.005

Thin films for structural tests in the FEI TITAN 80–300 high-resolution transmission electron microscope were cut from samples of the analyzed steel on a precision cutter. Then they were mechanically thinned on SiC sandpaper to a thickness of about 60 μm, and finally, ion beam polishing. Structural and diffraction studies were performed in the S/TEM FEI Titan 80–300 microscope at a voltage of 300 kV, equipped with a CESCOR Cs-probe corrector from CEOS Company (Corrected Electron Optical Systems GmbH) for STEM (scanning transmission electron microscopy) operation and an EDAX EDS spectrometer. To analyze the structure and diffraction of the tested steel, the following research techniques were used: BF (bright field), DF (dark field), SAED (selected area electron diffraction), HAADF (high angle annular dark field), HRTEM (*high-resolution TEM)*. In SAED studies, the parameters were as follows: condenser aperture C2–50 and camera length of 215–330. The convergence angle in STEM mode was 24 mrad.

The main goal of the research was to reveal the mechanisms determining the strengthening of the X98 and X105 steel during their thermo-mechanical treatment, which are reflected in the structure and properties of the analyzed steel.

3. RESULTS AND DISCUSSION

The results of tests in the transmission electron microscope in CTEM mode (conventional TEM) of X98 and X105 steel after the hot rolling show the occurrence of various deformation effects in their structure, such as shear bands, micro bands, and lens twins (Figs. 2 and 3). It was found that the micro bands intersect at an angle of ∼65°, and the size of the observed sub-grains is about 200 nm (Fig. 2a and 2d). The occurrence of the above-mentioned deformation effects is responsible for the strengthening of the structure, the strengthening of the tested steel, and the increase in their

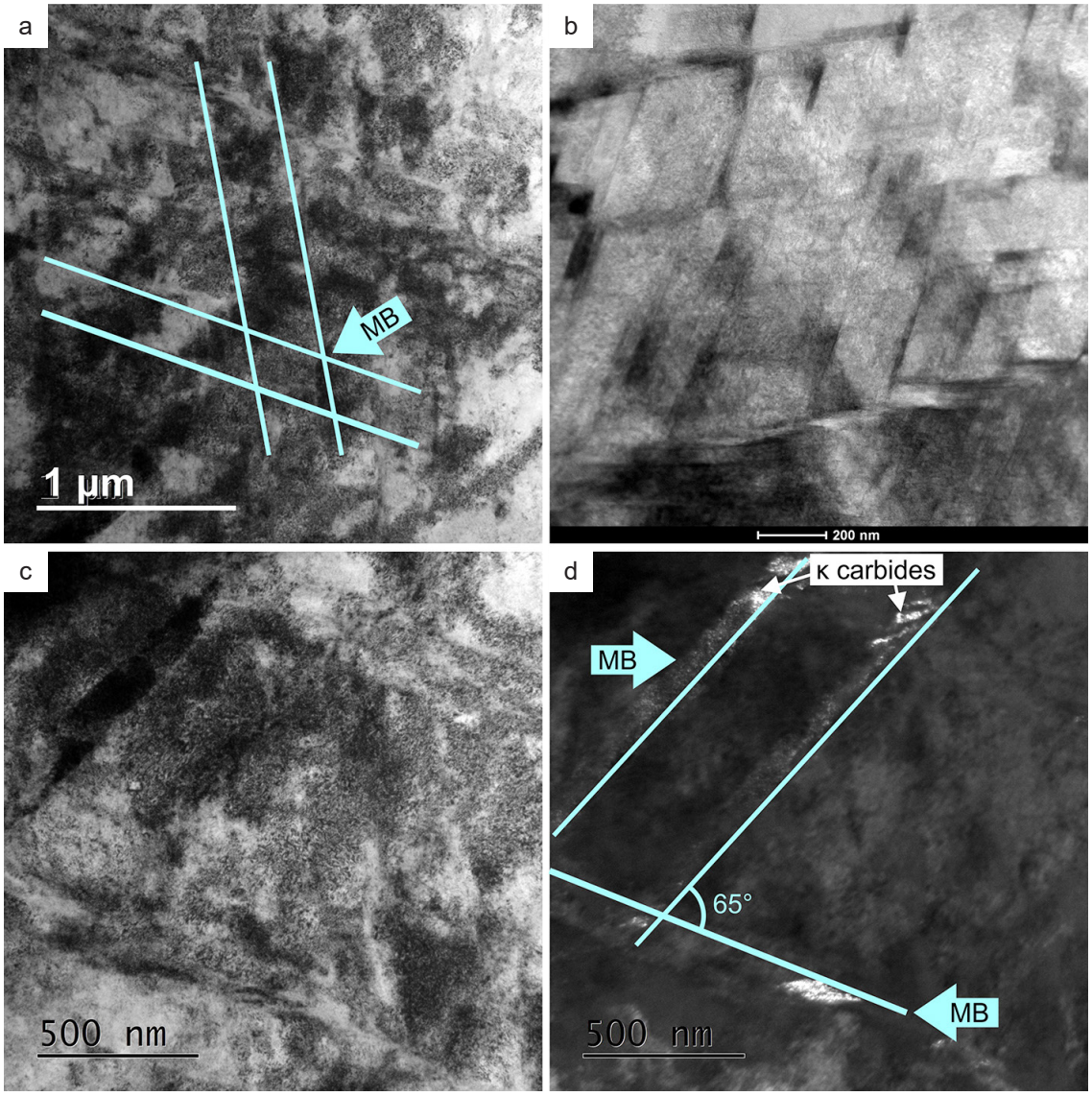

Fig. 2. The structure of hot-rolled X98 steel with micro bands in two systems – MBIP effect; a) and c) TEM BF; b) STEM BF and d) CTEM DF from the area in Fig. 2c of austenite reflex [111]; MB – micro band

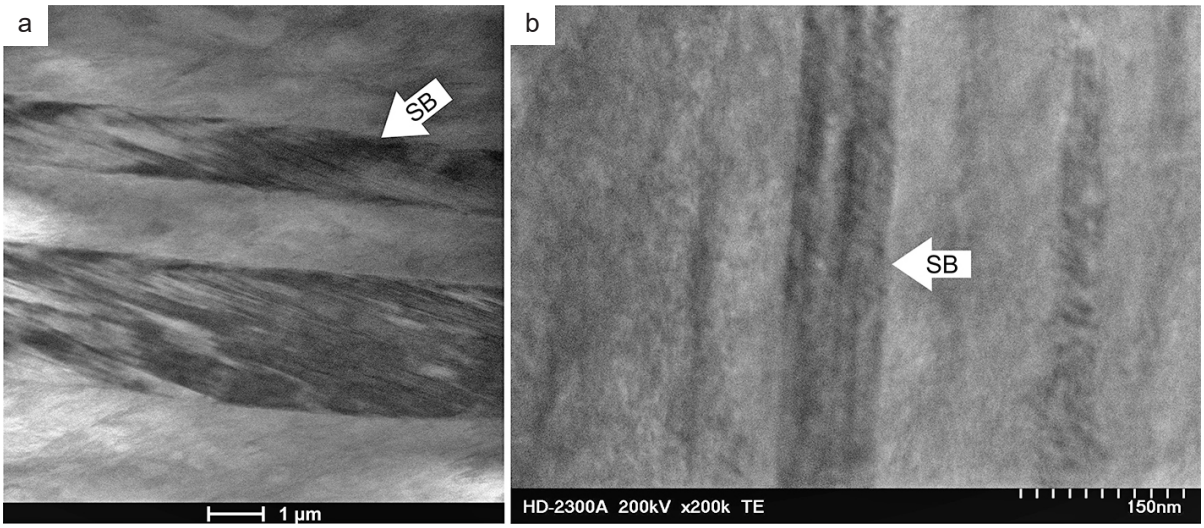

Fig. 3. Banding structure in steel a) X98 and b) X105 hot-rolled (STEM BF) – SIP effect, SB – shear band

strength properties. The shear bands are visible (Fig. 2a). The structure banding was also found in both tested types of steel, which is shown in Fig. 3.

The structure of X105 steel after thermo-mechanical treatment observed in the bright field is characterized by extinction contours, which mainly indicate the deformation of the network in the analyzed sample of the tested material (Fig. 4a). The STEM analysis allowed the observation of lens-shaped twins and the shear bands passing through them (Fig. 4b).

Based on transmission electron microscopy tests, it was found that the hardening mechanism of X98 and X105 steel is strain-induced plasticity by the formation of shear bands (SIP) (Fig. 3) and micro shear bands (MBIP) (Figs. 2 and 4). This is evidenced by the mutually intersecting 65° shear bands visible in the TEM microstructure. Shear bands generally occur in the high strain range and are the result of high localized plastic flow. The formation of shear bands is related to the avalanche slippage of dislocations across many grains and often across the entire cross-section of the polycrystalline material. Shear bands and the places of intersection of the bands with grain boundaries are areas of locally very high energy. According to the literature reports [3, 7, 10–12], it was confirmed that in the shear bands and micro bands as well as in the slip bands of the tested steel, κ carbides coherent with the matrix were observed (Figs. 2d, 5, 6 and 8), which hinder the movement of dislocation. The influence of κ carbides on the structure and properties was described in previous publications [4, 6, 19].

Tests in the transmission electron microscope were also carried out on steel samples after hot rolling and dynamic deformation with strain rates of 250 s^{-1} and 1000 s^{-1}. In X98 steel, after deformation at a speed of 250 s^{-1}, strong deformation effects such as clustering of dislocations or slip bands were observed. The slip bands, as in the steel structure, after rolling intersect at an angle of 65°, and their width is ~200 nm (Fig. 7). In the X98

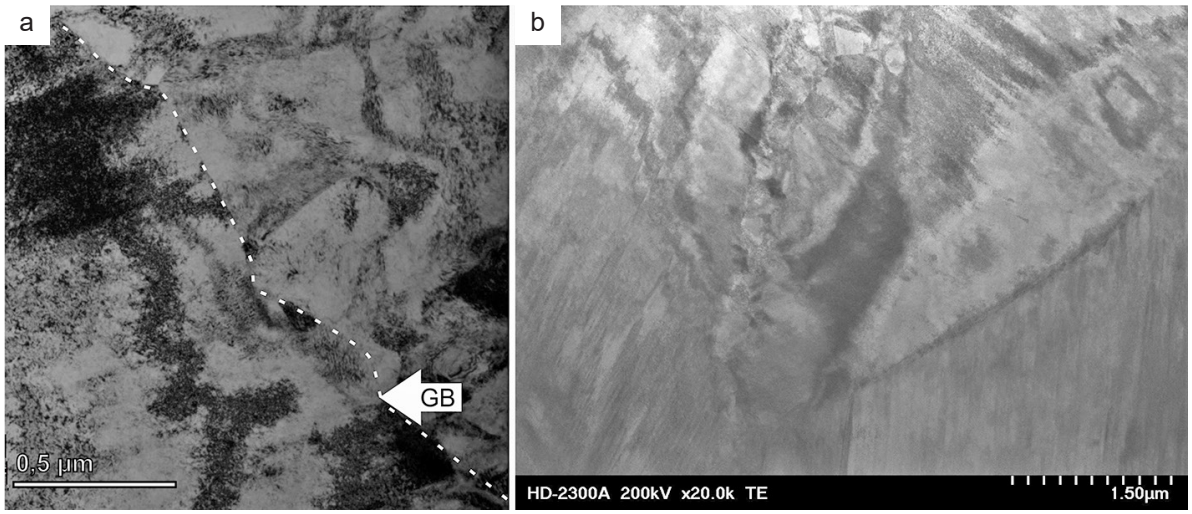

Fig. 4. The structure of X105 steel after hot rolling with a) numerous plastic deformation effects and extinction contours (STEM BF); b) lens-shaped twins and micro bands – MBIP effect (STEM BF), GB – grain boundary

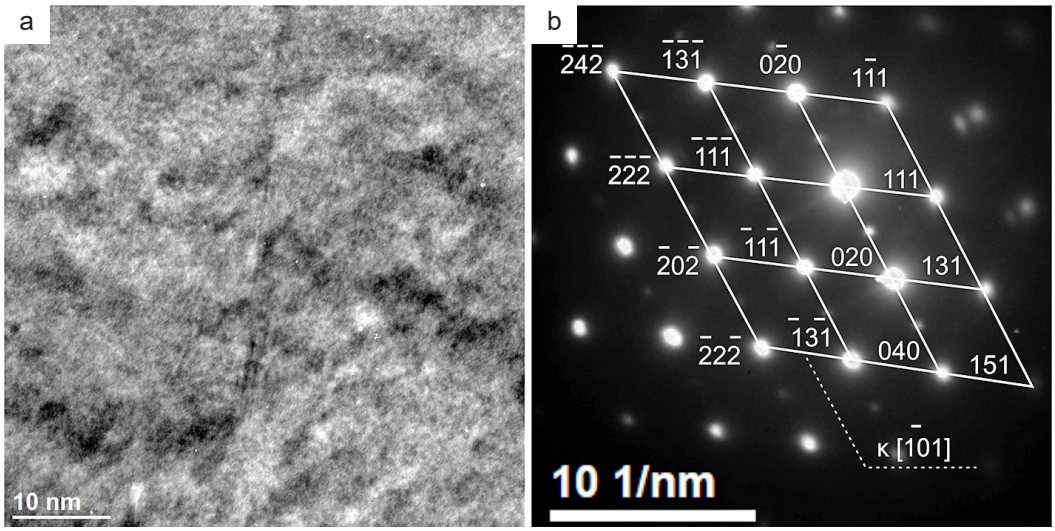

Fig. 5. The structure of hot-rolled X98 steel with κ carbide precipitation: a) TEM BF); b) diffraction from Fig. 5a with a partial solution – κ carbide with a zone axis [$\bar{1}$01]

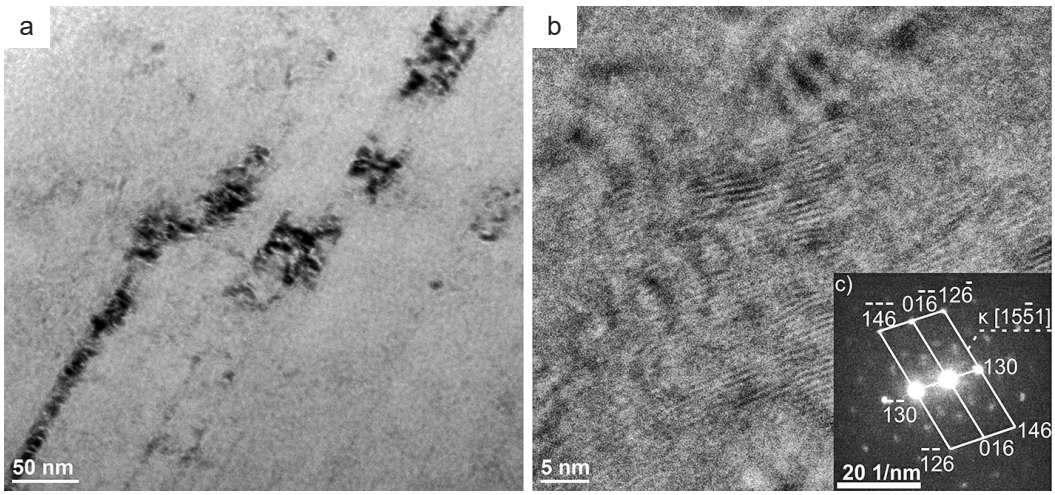

Fig. 6. The structure of hot-rolled X105 steel with κ carbide precipitation: a) TEM BF; b) HRTEM; c) diffraction from Fig. 6b with a partial solution – κ carbide with a belt axis [15$\bar{5}$1]

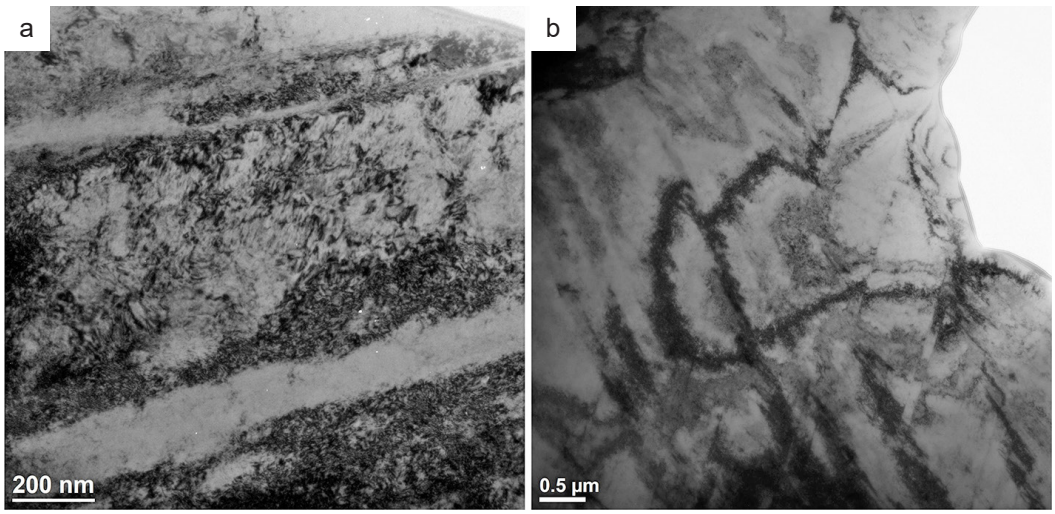

Fig. 7. Structure of hot-rolled X98 steel after dynamic deformation speed 250 s^{-1} a, b) TEM BF

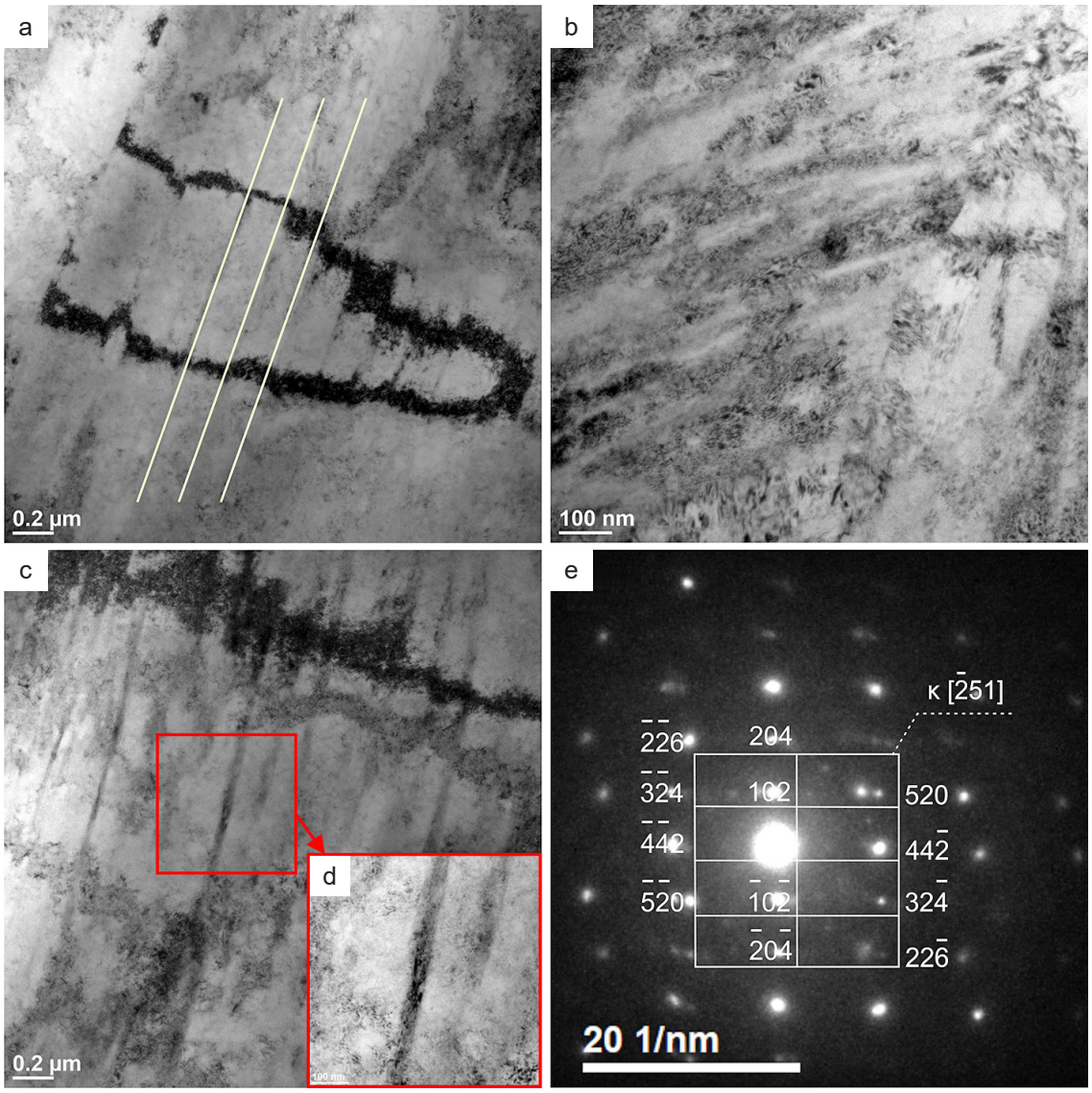

Fig. 8. Structure of hot-rolled X105 steel after dynamic deformation speed 1000 s^{-1} with visible slip bands – DSBR effect: a–d) TEM BF; e) diffraction from Fig. 8d with a partial solution – carbide κ with a belt axis [$\bar{2}$51]

and X105 steel, after deformation at a speed of 1000 s^{-1}, very narrow slip bands were observed, indicating a strong plastic deformation (Fig. 8). These bands intersect at an angle of 65° and their width is ~50 nm (Fig. 6).

4. CONCLUSIONS

In this study, it was confirmed based on TEM research that in TRIPLEX X98 and X105 steel the structural mechanisms determining the high mechanical properties of the steel during static deformation include strain-induced plasticity by shear band formation (SIP) and micro bands (MBIP). It was found that the micro shear bands intersect at an angle of ~65°, and the size of the sub-grains is about 200 nm.

In both tested types of steel slip bands with a width much smaller than during static deformation at the level of ~50 nm were identified in the microstructure after dynamic deformation, which was related to the plasticity induced by deformation and the formation of dynamic slip bands (DSBR).

Based on the results presented in this work, as well as the results already published [4–6, 19, 28, 29], it was found that in X98 and X105 steel nanometric κ-$(Fe, Mn)_3AlC$ carbides are located inside the austenite and ferrite grains, as well as at the grain boundaries. In X98 steel, the size of the κ carbide was much smaller than in X105 steel and ranged from a few to 160 nm, while in X105 steel, the κ carbides had a size from a few nanometers to even 1 μm. Nanometric κ carbides and their interaction with dislocations play a key role in strengthening TRIPLEX steel. It was confirmed that κ carbides which are coherent with the matrix, which hinders the dislocation movement, are located in the shear bands and microstrips as well as the slip bands in the tested steel. It has been found that κ carbides both block the movement of dislocation and are the source of their nucleation.

ACKNOWLEDGEMENTS

The article was written based on the results of the research described in the doctoral dissertation of Ms. Liwia Sozańska-Jędrasik entitled "Structure and properties of newly developed TRIPLEX high-manganese steel." Scientific work was financed as part of the project funded by the National Science Centre based on the decision number DEC-2012/05/B/ST8/00149.

REFERENCES

[1] M. Bausch, G. Frommeyer, H. Hofmann, E. Balichev, M. Soler, M. Didier, and L. Samek, *Ultra high-strength and ductile FeMnAlC light-weight steels*, European Commission Research Fund for Coal and Steel; Final Report Grant Agreement RFSR-CT-2006-00027, 2013.

[2] Y. Kimura, K. Hayashi, K. Handa, and Y. Mishima, "Microstructural control for strengthening the γ-Fe/E2$_1$–(Fe, Mn)$_3$AlC$_x$ alloys," *Mater. Sci. Eng. A*, vol. 329, no. 331, pp. 680–685, 2002.

[3] K. Eipper, G. Frommeyer, W. Fussnegger, and A.K.W. Gerick, *High-strength DUPLEX/TRIPLEX steel for lightweight construction and use thereof*, U.S. Patent 20070125454A1, 2002.

[4] L. Sozańska-Jędrasik, *Structure and properties of newly developed TRIPLEX high-manganese steels (title in Polish: Struktura i własności nowoopracowanych stali wysokomanganowych typu TRIPLEX)*, PhD. Thesis, Silesian University of Technology, Gliwice, Poland 2020, [in Polish].

[5] L. Sozańska-Jędrasik, J. Mazurkiewicz, W. Borek, and K. Matus, "Carbides analysis of the high strength and low density Fe-Mn-Al-Si steels," *Arch. Metall. Mater.*, vol. 63, no. 1, pp. 265–276, 2018.

[6] L. Sozańska-Jędrasik, J. Mazurkiewicz, K. Matus, and W. Borek, "Structure of Fe-Mn-Al-C Steels after Gleeble Simulations and Hot-Rolling," *Materials*, vol. 13, no. 3, p. 739, 2020.

[7] G. Frommeyer and U. Brüx, "Microstructures and mechanical properties of high-strength Fe-Mn-Al-C light-weight TRIPLEX steels," *Steel Res. Int.*, vol. 77, no. 9–10, pp. 627–633, 2006.

[8] M. Jabłońska, "*Struktura i Właściwości Austenitycznej Stali Wysokomanganowej Umacnianej Wskutek Mechanicznego Bliźniakowania w Procesach Dynamicznej Deformacji*," Publishing house of the Silesian University of Technology (Wydawnictwo Politechniki Śląskiej), Gliwice, Poland, 2016, [in Polish].

[9] S. Chen, R. Rana, A. Haldar and R.K. Ray, "Current state of Fe-Mn-Al-C low density steels," *Prog. Mater. Sci.*, vol. 89, pp. 345–391, 2017.

[10] A. Grajcar, "Nowoczesne stale wysokowytrzymałe dla motoryzacji II generacji," *STAL Metale & Nowe Technologie*, vol. 7–8, no. 10–13, pp. 10–13, 2013, [in Polish].

[11] S.S. Sohn *et al.*, "Novel ultra-high-strength (ferrite + austenite) duplex lightweight steels achieved by fine dislocation substructures (Taylor lattices), grain refinement, and partial recrystallization," *Acta Mater.*, vol. 96, pp. 301–310, 2015.

[12] M.C. Ha, J.M. Koo, J.K. Lee, S.W. Hwang and K.T. Park, "Tensile deformation of a low density Fe–27Mn–12Al–0.8C duplex steel in association with ordered phases at ambient temperature," *Mater. Sci. Eng. A*, vol. 586, pp. 276–283, 2013.

[13] U. Brüx, G. Frommeyer, and J. Jimenez, "Light-weight steels based on iron-aluminium – Influence of micro alloying elements (B, Ti, Nb) on microstructures, textures and mechanical properties," *Steel Res.*, vol. 73, no. 12, pp. 543–548, 2002.

[14] J.D. Yoo and K.T. Park, "Microband-induced plasticity in a high Mn–Al–C light steel," *Mater. Sci. Eng. A*, vol. 496, no. 1–2, pp. 417–424, 2008.

[15] J.D. Yoo, S.W. Hwang, and K.T. Park, "Origin of extended tensile ductility of a Fe-28Mn-10Al-1C steel," *Metall. Mater. Trans. A*, vol. 40, no. 7, pp. 1520–1523, 2009.

[16] E. Welsch *et al.*, "Strain hardening by dynamic slip band refinement in a high-Mn lightweight steel," *Acta Mater.*, vol. 116, pp. 188–199, 2016.

[17] L.A. Dobrzański, W. Borek, and J. Mazurkiewicz, "Influence of high strain rates on the structure and mechanical properties of high-manganes austenitic TWIP-type steel," *Materialwiss. Werkstofftech.*, vol. 47, no. 5–6, pp. 428–435, 2016.

[18] L.A. Dobrzański, W. Borek, and J. Mazurkiewicz, „Mechanical properties of high-Mn austenitic steel tested under static and dynamic conditions," *Arch. Metall. Mater.*, vol. 61, no. 2, pp. 725–730, 2016.

[19] L. Sozańska-Jędrasik, J. Mazurkiewicz, W. Borek, and L.A. Dobrzański, "Structure and phase composition of newly developed high manganese X98MnAlSiNbTi24–11 steel of TRIPLEX type," *Inżynieria Materiałowa*, vol. 2, no. 216, pp. 69–76, 2017.

[20] R. Ebner, P. Gruber, W. Ecker, O. Kolednik, M. Krobath, and G. Jesner, "Fatigue damage mechanisms and damage evolution near cyclically loaded edges," *Bull. Pol. Acad. Sci. Tech. Sci.*, vol. 58, no. 2, pp. 267–279, 2010.

[21] W. Borek, T. Tanski, Z. Jonsta, P. Jonsta, and L. Cizek, "Structure and mechanical properties of high-Mn TWIP steel after their thermo-mechanical and heat treatments" in Proc. *METAL 2015: 24th International Conference on Metallurgy and Materials*, Brno, Czech Republic, 2015, pp. 307–313.

[22] M. Sroka, A. Zieliński, and J. Mikuła, "The service life of the repair welded joint of Cr Mo/Cr-Mo-V," *Arch. Metall. Mater.*, vol. 61, no. 3, pp. 969–974, 2016.

[23] M. Sroka, M. Nabiałek, M. Szota, and A. Zieliński, "The influence of the temperature and ageing time on the NiCr23Co12Mo alloy microstructure," *Rev. Chim.*, vol. 4, pp. 737–741, 2017.

[24] T. Tomaszewski, P. Strzelecki, M. Wachowski, and M. Stopel, "Fatigue life prediction for acid-resistant steel plate under operating loads," *Bull. Pol. Acad. Sci. Tech. Sci.*, vol. 68, no. 4, pp. 913–921, 2020.

[25] A. Zieliński, M. Sroka, and T. Dudziak, "Microstructure and Mechanical Properties of Inconel 740H after Long-Term Service," *Materials*, vol. 11, p. 2130, 2018.

[26] L.A. Dobrzański and W. Borek, "Hot-Working Behaviour of Advanced High-Manganese C-Mn-Si-Al Steels," *Mater. Sci. Forum*, vol. 654–656, no. 1–3, pp. 266–269, 2010.

[27] M. Opiela, G. Fojt-Dymara, A. Grajcar, and W. Borek, "Effect of Grain Size on the Microstructure and Strain Hardening Behavior of Solution Heat-Treated Low-C High-Mn Steel," *Materials*, vol. 13, no. 7, p. 1489, 2020.

[28] L. Sozańska-Jędrasik, J. Mazurkiewicz, and W. Borek, "The influence of the applied type of cooling after eight-stage hot compression test on the structure and mechanical properties of TRIPLEX type steels," *MATEC Web Conf.*, vol. 252, p. 08005. 2019.

[29] L. Sozanska-Jedrasik, J. Mazurkiewicz, W. Borek, K. Matus, B. Chmiela, and M. Zubko, "Effect of Nb and Ti micro-additives and thermo-mechanical treatment of high-manganese steel with aluminium and silicon on their microstructure and mechanical properties," *Arch. Metall. Mater.*, vol. 64, no. 1, pp. 133–142, 2019.